Journal of Photochemistry and Photobiology A: Chemistry 221 (2011) 164–168

Contents lists available at ScienceDirect

Journal of Photochemistry and Photobiology A: Chemistry

journal homepage: www.elsevier.com/locate/jphotochem

# Plasmon coupling and coherent acoustic phonon dynamics of periodic gold pair nanocuboids by near-IR transient absorption spectroscopy

Li Wang[a], Yoshiaki Nishijima[b], Kosei Ueno[b], Hiroaki Misawa[b], Naoto Tamai[a,*]

[a] Department of Chemistry, School of Science and Technology, Kwansei Gakuin University, Japan
[b] Research Institute for Electronic Science, Hokkaido University, Japan

ARTICLE INFO

*Article history:*
Available online 26 February 2011

*Keywords:*
Plasmon coupling
Coherent acoustic phonon
Gold nanocuboid
Near-IR transient absorption spectroscopy

ABSTRACT

Gold pair nanocuboids (size: 150 nm × 150 nm × 20 nm) with different nanogaps ranging from 0 to 10.6 nm were prepared by the electron-beam lithography. Effect of plasmon coupling on coherent acoustic phonon dynamics of gold pair nanocuboids was examined as a function of nanogaps by near-IR transient absorption spectroscopy at 400-nm excitation. The similar oscillation periods of coherent acoustic phonon vibration (88 ± 1 ps) were observed for all the gold pair nanocubiods irrespective of the nanogaps, which was analyzed by the oscillation of bleaching peaks of SPR bands and the transient absorption dynamics. The coherent acoustic phonon vibration of gold nanocuboids was only influenced by the nanostructure itself, even though SPR band was much influenced due to the dipole coupling between the adjacent Au nanocuboids. In addition, it was revealed that the electron–phonon coupling (~0.7 ps) was followed by the initial size change of gold nanocuboid with the time scale that was a little slower (~1.7 ps) than the electron–phonon coupling.



## 1. Introduction

Surface-plasmonic metal nanostructures have shown their dazzling optical properties in the applications of surface-enhanced spectroscopies, biological and chemical sensing, and nanophotonic devices, which interactively excite the researches in tailoring and fine-tuning their optical properties by various fabricating methods [1–4]. Surface plasmon resonance (SPR) bands of metal nanostructures depend on the size, the shape, the dielectric properties of the surroundings as well as electromagnetic particle interactions of the nearby metal nanostructures [5]. With the help of nanofabrication methods, such as electron beam lithography (EBL), the size and the structure of metal nanoparticles can be efficiently and precisely controlled with nanoscale resolution and the relationship between SPR band and the nanogap of the metal nanoparticle dimer can be clearly presented [6]. The SPR band of nanoparticle dimer is exponentially red-shifted with the decrease of the gap between the two nanoparticles due to near field coupling, which follows the "plasmon ruler equation" $\Delta\lambda/\lambda_0 \sim k \times \exp(-s/\tau D)$ ($\lambda_0$ is the SPR band of single metal nanoparticle, $\Delta\lambda$ is the shift of SPR band of the dimer, $k$ is a constant, $s$ is the central separation between the two nanoparticles, $\tau$ is the decay constant and approximately 0.2, and $D$ is one particle dimension) [7–9].

Under the ultrafast excitation, the metal nanostructures experience the following processes: the electron–electron scattering (a few hundred fs), electron–phonon coupling (a few ps) and the thermal energy transfer to environments (a few hundred ps) [2,10–12]. The time-resolved measurements of metal nanostructures can provide the physical properties of electron, phonon and also the elastic properties. The relationships between the coherent acoustic phonon vibration and the particle size, shape, crystal structure and the local environment have been characterized for the colliod and single metal nanoparticles [13–17]. However, the influence of the dipole coupling between the metal dimer on the coherent acoustic phonon vibration is still less studied, which was mainly reported by El-sayed's group. They found that the dipole coupling can influence both the SPR bands and the phonon oscillation of the metal nanoparticles [18,19]. For example, the studies of silver and gold monolayer nanoprism arrays prepared by nanosphere lithography presented a slight deviation of the observed oscillation periods from the calculated values that was assigned to the influence of the dipole coupling [18]. Furthermore, they presented that a fractional shift in the oscillation frequency follows an exponential decay with respect to the interparticle gaps scaled by the particle diameter on the studies of coherent lattice phonon oscillation in electron-beam fabricated gold nanoparticle pairs [19]. The fractional shift in the oscillation frequency was 5 times larger than that of the SPR band for the gold nanoparticle pair and assigned to a reflection of the near-field coupling. However, in our pervious report, we examined the coherent acoustic phonon vibration of periodic single and pair of gold nanocuboids by femtosecond near-IR transient absorption

* Corresponding author. Tel.: +81 79 565 8357; fax: +81 79 565 8357.
*E-mail address:* tamai@kwansei.ac.jp (N. Tamai).

1010-6030/$ – see front matter © 2011 Elsevier B.V. All rights reserved.
doi:10.1016/j.jphotochem.2011.02.023

spectroscopy and found that the SPR band was influenced by the near field coupling of the nanocuboids while the oscillation period of the coherent acoustic phonon was almost the same for the single and the pair [20]. To examine the effects of the interparticle interaction much more carefully, we prepared a series of the gold pair nanocuboid arrays and performed femtosecond near-IR transient absorption measurements. The coherent acoustic phonon vibration of the dimers with different nanogap separations was discussed by examining the dynamics at bleaching wavelength, the oscillation of bleaching peaks and the excitation intensity dependence.

## 2. Materials and methods

All the arrays studied in this work consist of gold pair nanocuboids patterned on quartz slides by EBL (ELS-7700H, Elionix Co., Ltd., Japan) with overall dimensions of 30 μm × 30 μm as shown in Fig. 1 [21,22]. The patterns are characterized by field-emission scanning electron microscopy (FE-SEM) apparatus (JEOL JSM-6700FT) with 1-nm resolution. Fig. 1a shows a typical FE-SEM image of the pairs, in which the size of one gold nanocuboid is 150 nm × 150 nm × 20 nm. The nanogap within one pair (the distance between the vertexes of the gold nanocuboids) is 10.6 nm and the center-to-center separation between two pairs is 400 nm. For the series of gold pair nanocuboids, the designed nanogap separations are 0, 1.8, 3.5, 5.3, 7.1, 8.8 and 10.6 nm, respectively.

Transient absorption (TA) spectra were measured with a conventional pump-probe method. The pump beam was second harmonic of an amplified Ti: sapphire laser (Spectra-physics, 1 kHz, 80 fs, 800 nm), and the probe beam was super-continuum generated by focusing a fundamental laser beam into a sapphire plate. The polarization of pump and probe beams was rotated to the direction of the long diagonal line of the pair, which was marked as +45° in Fig. 1b. The signal and the reference beams in near-IR spectral region were controlled using a chopper in the pump-light path with 500 Hz repetition rate and detected by an InGaAs detector (Princeton Instruments, OMA V). The sample position was precisely optimized in a three-dimensional holder and monitored by a telescope. The steady-state extinction spectra were calculated using the logarithmic function of the quotient of the white light intensities with and without the sample.

## 3. Results and discussion

The normalized extinction spectra with +45° polarization direction of the incident light are shown in Fig. 2a, and their peak wavelengths and the FWHM of SPR bands are summarized in Fig. 2b. The inset in Fig. 2a is the extinction spectra with −45° polarization direction of the incident light (orthogonal to +45° polarization direction, marked as −45°). The +45° SPR bands in Fig. 2a show a remarkable red-shift from 975 nm to 1050 nm and the band width (FWHM) becomes broader from 1600 $cm^{-1}$ to 2255 $cm^{-1}$ (151–245 nm) with the decrease of the nanogap separation from 10.6 nm to 0 nm. In the inset of Fig. 2a, the −45° SPR bands are almost constant with the peak at 865 nm irrespective of the different nanogap separation. The red-shift of SPR bands with the decrease of the nanogap can be explained by enhancing the restoring forces for the plasma electrons due to the presence of the charge distribution of the neighbouring particle [8]. Because the interdimer separation is only 400 nm, the SPR band of the gold pair nanocuboids should consider the near-field coupling effects from interparticle and interdimer. Although the shift of the SPR bands does not give a good fitting with the exponential decay function $\Delta\lambda/\lambda_0 = k \times \exp(-s/\tau D)$, the shift of the SPR bands with the change of nanogap separation can be clearly detected.

**Table 1**
The fitting results of the transient absorption measurements for gold pair nanocuboids with different nanogaps by two exponential decays plus a damped cosine function: $T_{\Delta OD}$ and $T_{bleaching}$ are the oscillation periods obtained from the decay profiles and the oscillation of bleaching peaks; $\tau_{e-p,\Delta OD}$ and $\tau_{e-p,bleaching}$ are the lifetimes for electron–phonon coupling.

| Nanogap (nm) | $T_{\Delta OD}$ (ps) | $\tau_{e-p,\Delta OD}$ (ps) | $T_{bleaching}$ (ps) | $\tau_{e-p,bleaching}$ (ps) |
|---|---|---|---|---|
| 0 | 87.5 | 0.67 | 88.9 | 1.44 |
| 1.8 | 88.2 | 0.69 | 88.9 | 1.65 |
| 3.5 | 87.3 | – | 86.3 | – |
| 5.3 | 88.2 | 0.71 | 88.6 | 1.87 |
| 7.1 | 88.3 | 0.73 | 88.9 | 1.7 |
| 8.8 | 88.9 | 0.72 | 88.3 | 1.72 |
| 10.6 | 88.5 | 0.80 | 88.0 | 1.79 |

Fig. 3 shows the result of TA measurements for the pair with 10.6-nm nanogap under the 200-nJ excitation and +45° polarization direction of probe pulses. In Fig. 3b, the transient absorption spectra at various delay times are illustrated. The bleaching peaks around 965 nm corresponds to the SPR band around 975 nm with the +45° polarization direction of probe pulses, in which the corresponding extinction spectrum is illustrated in Fig. 3a. Although the positive absorption signals were always stronger at the red sides, the absorption at the both sides of the bleaching band was observed. This is due to the broadening and red-shift of the SPR bands originating from the impulsive hot electrons and the heating of the lattice. At the longer delay-time scales, the shifts of the bleaching peaks can be observed, which reflects the oscillation of the SPR bands and thus the coherent acoustic phonon vibration. Fig. 3c illustrates the decay profiles at 940 and 1060 nm corresponding to the two sides of the SPR band. The slowly damped oscillations were ~180° out-of-phase for the two curves and similar to the cases of gold nanorods and spherical particles [13,23]. As mentioned in the introduction, the dynamics for the processes of electron–phonon coupling (subscript *e–p*), phonon vibrations (subscript *ν*) and thermal coupling to the environment (subscript *th*) can be expressed with the following equation:

$$R(t) = A_{e-p}\exp\left(\frac{-t}{\tau_{e-p}}\right) + A_{\nu}\exp\left(\frac{-t}{\tau_{\nu}}\right)\cos\left(\frac{2\pi t}{T_{\nu}} + \varphi_{\nu}\right) + A_{th}\exp\left(\frac{-t}{\tau_{th}}\right) \quad (1)$$

The initial electron–electron scattering was omitted in our analysis. In Fig. 3c, the decay profiles were fitted with the equation (1), and the oscillation periods at both wavelengths were calculated to be 86.4 and 88.7 ps, respectively. The oscillation of the bleaching peaks is illustrated in Fig. 3d, in which the peak wavelengths were obtained by fitting with Gaussian functions to the transient absorption spectra at different delay times. The oscillation period was obtained to be 88.3 ps in accordance with the oscillation periods of the decay profiles in Fig. 3c.

Fig. 4 illustrates the decay profiles at bleaching wavelengths and the oscillation of bleaching peaks for the gold pair nanocuboids with different nanogaps under the 200-nJ excitation and +45° polarization direction of the probe pulse. As clearly shown in Fig. 4a, a similar vibrational frequency was observed for the pairs with different nanogaps. A similar vibrational behavior was also observed in the dynamics of bleaching peak shift as illustrated in Fig. 4b. The wavelengths of the bleaching peaks showed oscillatory shifts, which correspond to the periodic shift of SPR bands. The solid lines in Fig. 4 are the fitting results by using Eq. (1). All of the vibrational frequencies of nanocuboid dimers with different nanogaps were summarized in Table 1, and the oscillation periods obtained from ΔOD ($T_{\Delta OD}$) and the bleaching peak shift ($T_{bleaching}$) were ~88 ps irrespective of the nanogap separation. From these results, it can be clearly shown that the dipole coupling of the pair only influences

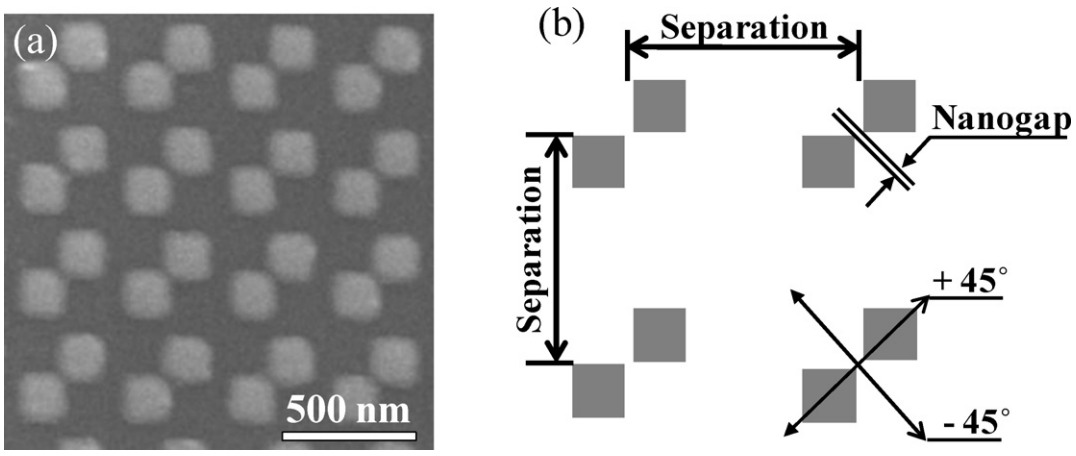


**Fig. 1.** SEM image (a) and representative scheme (b) of gold pair nanocuboids with 400-nm separation and 10.6-nm nanogap. The polarization direction of the long diagonal line of the pair was marked as +45° in (b) and its vertical direction as −45°.

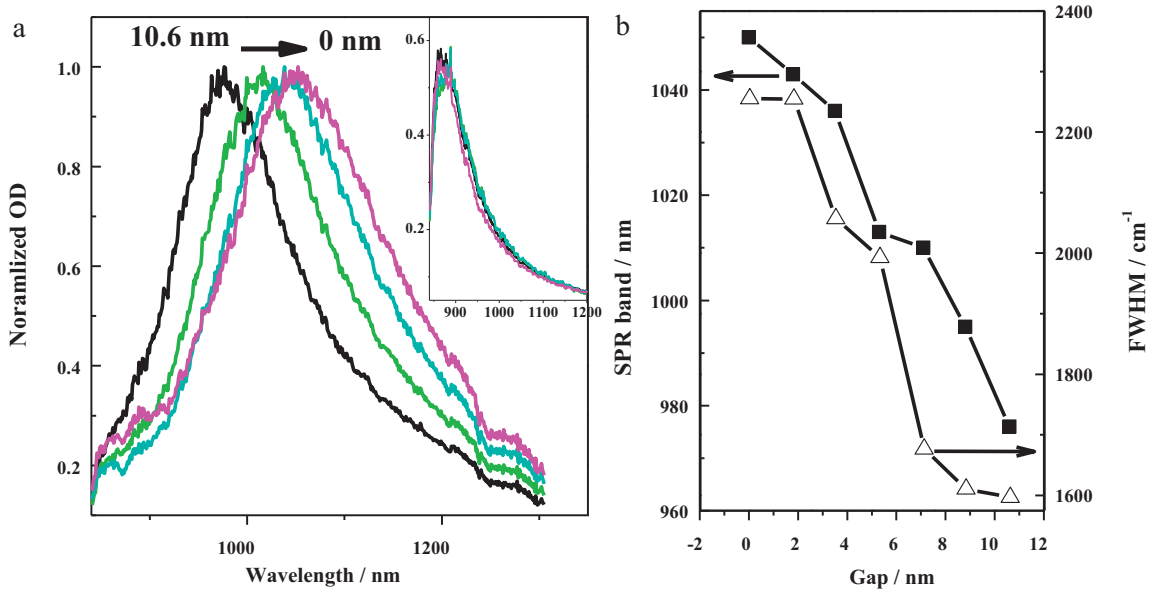


**Fig. 2.** The normalized extinction spectra (a) with +45° polarization direction of the incident light and (inset) with −45° polarization direction of the incident light for the gold pair nanocuboids with different nanogaps of 10.6, 7.1, 3.5 and 0 nm. (b) The relationship between the nanogaps and the SPR bands (filled square) or the FWHM (empty triangle).

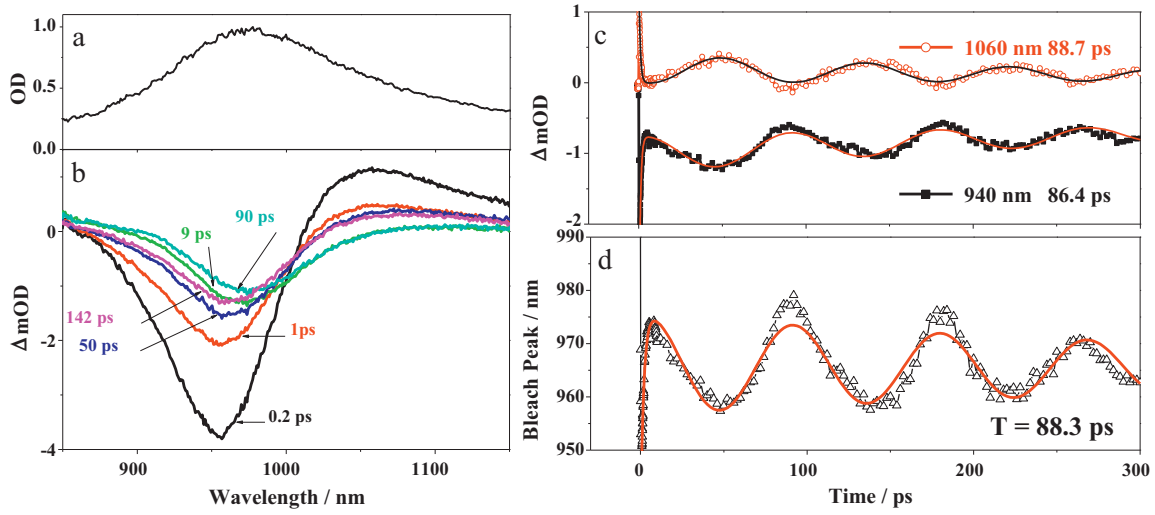


**Fig. 3.** Transient absorption measurements for 10.6-nm nanogaped gold pair nanocuboids with +45° polarization direction of the incident light. (a) The extinction spectrum. (b) The transient absorption spectra at different delay times of 0.2, 1, 9, 50, 90 and 142 ps. (c) The decay profiles of 940 nm (filled square) and 1060 nm (empty circle). The solid lines are the fitting results by two exponential decays plus a damped cosine function. (d) Oscillation of the bleaching peaks and its fitting result.

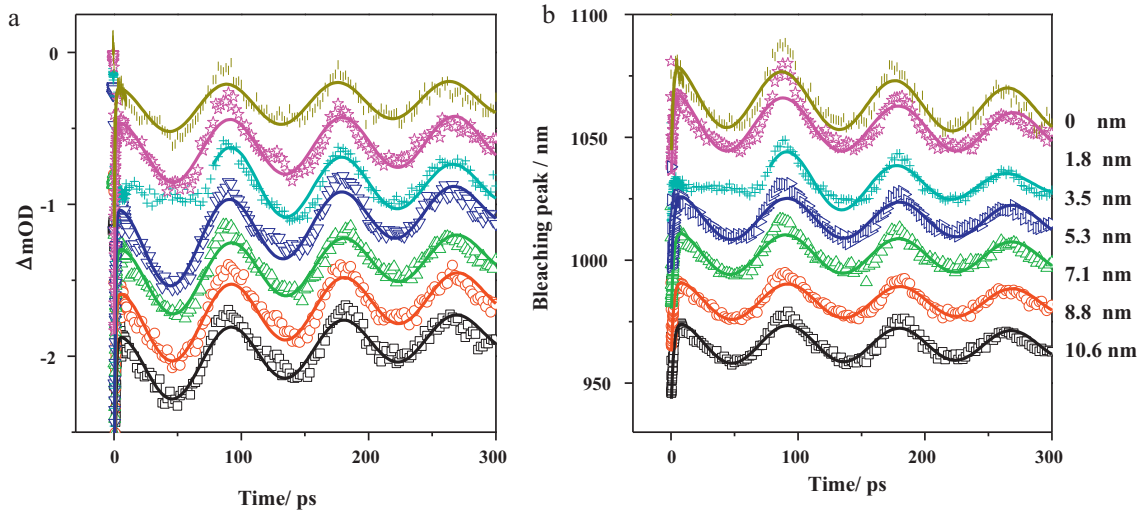


**Fig. 4.** The transient absorption measurements for the gold pair nanocuboids of different nanogaps from 0 to 10.6 nm with +45° polarization direction of the incident light: the decay profiles at bleaching wavelengths (a) and the oscillation of the bleaching peaks (b).

the SPR bands but not the coherent acoustic phonon vibrations. The result is in good agreement with Ref. [20]. As compared with the vibrational frequency of 77 ps in Ref. [20], the different height might be considered. In this paper, the height was designed to be ~20 nm while ~15 nm height was designed in Ref. [20]. Therefore, the coherent acoustic phonon vibration was only related with the intrinsic characters of gold nanocuboid, such as the size, the shape and the elastic properties while not influenced by the dipole coupling of the proximities.

However, the fractional frequency shift of coherent acoustic phonon vibration was observed for the gold nanodisc pair [19]. The circular gold nanodiscs with 88-nm diameter were examined at the selected one wavelength in transient absorption spectroscopy, in which the vibrational frequency may be influenced by the size dispersion of the system. The shift of the bleaching peak wavelength is more representative to detect the coherent acoustic phonon vibration of the whole system. The phonon vibration is mainly from the expansion and contraction of whole lattice of the gold nanocuboid while the electric field induced by the near field coupling is much enhanced in the tip region of the nanocuboid pair. The size and the shape of the nanostructures might be important factors of the dipole coupling effect. A systematical study of the dipole-coupling effect on the coherent acoustic phonon vibration with different particle size is necessary and in progress.

As summarized in Table 1, the lifetime of *e–p* coupling obtained from ΔOD ($\tau_{e-p,\Delta OD}$) is almost constant with a value of ~0.7 ps. The lifetime of *e–p* coupling is known to be dependent on the excitation intensity, and this value is in good agreement with $\tau_{e-p}$ of Au nanoparticles at low excitation intensity limit [24]. However, the lifetime of *e–p* coupling obtained from the bleaching peak shift ($\tau_{e-p,bleaching}$) is more than double and ~1.7 ps irrespective of the nanogap separation, in which the data were obtained from exactly the same transient absorption data as the estimation of $\tau_{e-p,\Delta OD}$. This fast component obtained from the bleaching peak shift represents the size change of the nanocuboid. Thus, the *e–p* coupling, the energy transfer from the electron to the lattice, is followed by the initial size change of nanocuboid with the time that is a little slower than the *e–p* coupling.

The excitation intensity dependence of the gold pair nanocuboids with 8.8-nm nanogap was examined. Fig. 5 shows the decay profiles at the bleaching wavelength with the excitation intensities of 200, 300 and 400 nJ/pulse. The oscillation amplitudes and the difference absorption (ΔOD) of the decay profiles linearly increase with the increase of excitation intensity as shown in

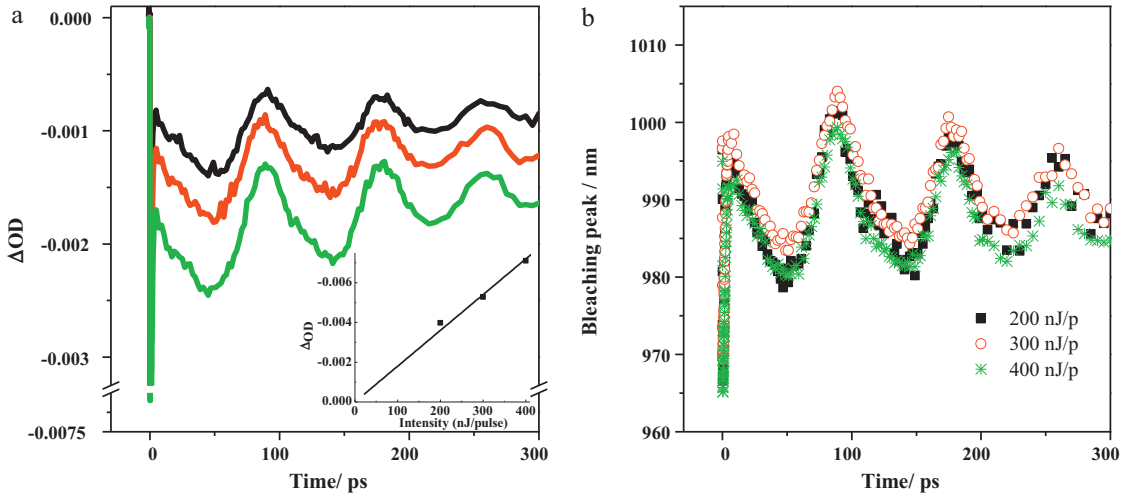


**Fig. 5.** Excitation intensity dependence of 8.8-nm nanogaped gold pair nanocuboids for the dynamics at the bleaching wavelength (a) and the oscillation of the bleaching peaks (b). The inset in (a) is the relationship of excitation intensity and the minimum ΔOD of the bleaching peak.

Fig. 5a and its inset. However, not only the central wavelengths but also the oscillation amplitudes of bleaching peaks in the vibrational processes were similar for the different excitation intensities as shown in Fig. 5b [25]. With the impulsive excitation of gold nanocuboids, the hot electrons and the heated lattice are responsible for the shift and broadening of the SPR bands and hence the coherent acoustic phonon vibrations. The SPR band shift and the phonon vibrations are related with the initial electron and phonon temperatures and hence the excitation intensity [24]. However, from our results, the coherent acoustic phonon vibrations are not influenced by the excitation intensity even though the absorbed photons are increased with the increase of excitation intensity.

## 4. Conclusion

We investigated the ultrafast dynamics of periodic gold nanocuboid dimers with different nanogap separations by femtosecond near-IR transient absorption spectroscopy. The SPR bands of the nanocuboid dimers were influenced by the near field coupling while the vibrational frequencies of the coherent acoustic phonons were almost the same for all of the dimers. The phonon vibration was only influenced by the intrinsic properties of the metal nanostructures, such as the size, the shape and the materials, but not the dipole coupling of the proximities. In addition, the excitation intensity dependence of coherent acoustic phonon vibration was examined. Although the amplitude of the absorption was linearly increased with the increase of excitation intensity, the amplitude of coherent acoustic phonon vibration of the bleaching peak shift was not influenced by the excitation intensity within the current intensity range. In addition, the experimental results revealed that the *e–p* coupling (∼0.7 ps) was followed by the initial size change of gold nanocuboid with the time scale that was a little slower (∼1.7 ps) than the *e–p* coupling.

## Acknowledgements

Acknowledgements are made to Grant-in-Aid for Scientific Research on Priority Areas of Strong Photon-Molecule Coupling Fields (No. 470) from MEXT, Japan, for support of this research.

## References

[1] X.M. Lu, M. Rycenga, S.E. Skrabalak, B. Wiley, Y.N. Xia, Annu. Rev. Phys. Chem. 60 (2009) 167.
[2] S. Link, M.A. Ei-Sayed, Annu. Rev. Phys. Chem. 54 (2003) 331.
[3] K.A. Willets, R.P. Van Duyne, Annu. Rev. Phys. Chem. 58 (2007) 267.
[4] J.N. Anker, W.P. Hall, O. Lyandres, N.C. Shah, J. Zhao, R.P. Van Duyne, Nat. Mater. 7 (2008) 442.
[5] B. Lamprecht, G. Schider, R.T. Lechner, H. Ditlbacher, J.R. Krenn, A. Leitner, F.R. Aussenegg, Phys. Rev. Lett. 84 (2000) 4721.
[6] J. Henzie, J. Lee, M.H. Lee, W. Hasan, T.W. Odom, Annu. Rev. Phys. Chem. 60 (2009) 147.
[7] K.H. Su, Q.H. Wei, X. Zhang, J.J. Mock, D.R. Smith, S. Schultz, Nano Lett. 3 (2003) 1087.
[8] W. Rechberger, A. Hohenau, A. Leitner, J.R. Krenn, B. Lamprecht, F.R. Aussenegg, Opt. Commun. 220 (2003) 137.
[9] P.K. Jain, W.Y. Huang, M.A. El-Sayed, Nano Lett. 7 (2007) 2080.
[10] W. Huang, M.A. El-Sayed, Eur. Phys. J. -Spec. Top. 153 (2008) 325.
[11] G.V. Hartland, Annu. Rev. Phys. Chem. 57 (2006) 403.
[12] G.V. Hartland, Phys. Chem. Chem. Phys. 6 (2004) 5263.
[13] M. Hu, X. Wang, G.V. Hartland, P. Mulvaney, J.P. Juste, J.E. Sader, J. Am. Chem. Soc. 125 (2003) 14925.
[14] L. Bonacina, A. Callegari, C. Bonati, F. van Mourik, M. Chergui, Nano Lett. 6 (2006) 7.
[15] H. Petrova, J. Perez-Juste, Z.Y. Zhang, J. Zhang, T. Kosel, G.V. Hartland, J. Mater. Chem. 16 (2006) 3957.
[16] A.L. Tchebotareva, M.A. van Dijk, P.V. Ruijgrok, V. Fokkema, M.H.S. Hesselberth, M. Lippitz, M. Orrit, ChemPhysChem 10 (2009) 111.
[17] P. Zijlstra, A.L. Tchebotareva, J.W.M. Chon, M. Gu, M. Orrit, Nano Lett. 8 (2008) 3493.
[18] W.Y. Huang, W. Qian, M.A. El-Sayed, J. Phys. Chem. B 109 (2005) 18881.
[19] W.Y. Huang, W. Qian, P.K. Jain, M.A. El-Sayed, Nano Lett. 7 (2007) 3227.
[20] L. Wang, Y. Nishijima, K. Ueno, H. Misawa, N. Tamai, Appl. Phys. Lett. 95 (2009) 053116.
[21] K. Ueno, S. Juodkazis, V. Mizeikis, K. Sasaki, H. Misawa, J. Am. Chem. Soc. 128 (2006) 14226.
[22] K. Ueno, V. Mizeikis, S. Juodkazis, K. Sasaki, H. Misawa, Opt. Lett. 30 (2005) 2158.
[23] G.V. Hartland, J. Chem. Phys. 116 (2002) 8048.
[24] J.H. Hodak, A. Henglein, G.V. Hartland, J. Chem. Phys. 111 (1999) 8613.
[25] A little shift of the central oscillation wavelength in Fig. 4b and Fig. 5b for the 8.8-nm nanogap pair was explained to the accuracy of the detected position on the samples.